REVIEW ARTICLE

Characterisation of brain disorders and evaluation of therapy by functional and molecular magnetic resonance techniques

YX Wang 王毅翔
Wynnie WM Lam 林慧雯

Objectives To review advanced functional and molecular magnetic resonance techniques that are currently clinically useful or with potential clinical use in the near future.

Data sources and extraction Literature search of Medline to December 2007 was conducted. Key words search terms were: 'magnetic resonance imaging', 'magnetic resonance spectroscopy', 'brain', 'functional', 'perfusion', 'diffusion', 'diffusion tensor', 'magnetic transfer', 'molecular imaging', 'superparamagnetic iron oxide'. Relevant original papers and review articles were retrieved.

Study selection A total of 83 original papers and review articles were systematically analysed.

Data synthesis The introduction of modern neuroimaging modalities in recent years has revolutionised investigation of the normal and diseased brain. Among others, magnetic resonance has emerged as the pre-eminent imaging modality, which can produce both high-resolution anatomical images and maps that reflect a variety of physiological parameters relevant to functional assessment and tissue characterisation. Magnetic resonance imaging techniques are now capable of visualising physiological and diseased processes at cellular and molecular levels, including cerebral blood flow, capillary perfusion and permeability, blood oxygenation level–dependent neuronal activation, microscopical motion of water (water diffusion), integrity of axonal fibres, and the molecular transfer of magnetisation within tissues. Magnetic resonance cell trafficking can evaluate the macrophage activity in areas of brain inflammation. Magnetic resonance cell-labelling strategies can be used to monitor the seeding and migration of embryonic stem cells. Magnetic resonance spectroscopy allows the detection of various metabolites that pertain to different biochemical processes in brain tissues. Such metabolites/spectra include: N-acetyl aspartate used as a neuronal marker, choline as a cell membrane metabolism marker, myo-inositol as a glial marker in proton spectrum, and phosphorous whose spectrum provides an in-vivo assessment of the bio-energetic status of tissues. Besides characterisation of brain disorders, magnetic resonance imaging and spectroscopy can improve the planning and monitoring of therapy and contribute to the development of new therapies.

Conclusion Advances in neuroimaging have made a great leap in the morphological, metabolic, and functional assessment of the neurological diseases, enabling better diagnosis and management of patients.

Key words
Brain; Diffusion; Magnetic resonance imaging; Magnetic resonance spectroscopy; Perfusion

Hong Kong Med J 2008;14:469-78

Department of Diagnostic Radiology and Organ Imaging, The Chinese University of Hong Kong, Prince of Wales Hospital, Shatin, Hong Kong
YX Wang, MMed, PhD
WWM Lam, MD, FRCR

Correspondence to: Prof YX Wang
E-mail: yixiang_wang@cuhk.edu.hk

Introduction

Magnetic resonance (MR) is based upon intrinsic magnetic properties of atomic nuclei with an odd number of protons and/or neutrons (eg ^{1}H, ^{13}C, and ^{31}P). The MR signal of an in-vivo MR spectrum (MRS) or image (MRI) is primarily dependent upon the nuclear spin density and the MR T1/T2 relaxation times. Magnetic resonance image generally refers to the spatial distribution of the ^{1}H (protons). The MRS enables detection of the minute differences in molecular resonance frequencies that indicate the chemical environment of

功能性及分子磁力共振技術應用於腦疾病診斷及治療效果評估的現狀

目的 綜述已經臨床應用或近期將應用於臨床的功能性磁力共振及分子磁力共振成像技術。

資料來源與選取 以'magnetic resonance imaging', 'magnetic resonance spectroscopy', 'brain', 'functional', 'perfusion', 'diffusion', 'diffusion tensor', 'magnetic transfer', 'molecular imaging', 'superparamagnetic iron oxide'為關鍵詞，檢索Medline資料庫2007年12月以前的相關論文和綜述文章。

研究選取 對83篇原始論文和綜述文章進行系統分析。

資料綜合 近年來現代神經影像技術發展迅速。磁力共振作為優越的成像工具，可以同時提供高分辨率的解剖圖像及參數圖像以反映與腦功能及組織特徵有關的生理參數。現代磁力共振能夠在細胞及分子水平觀察腦生理及疾病過程，包括測量腦血流、毛細血管灌注及通透性、神經細胞活動、水分子彌散、神經軸突完整性，以及組織中的分子磁性轉換。磁力共振細胞跟蹤技術可以評估腦炎癥區域的巨噬細胞活動狀況。磁力共振細胞標記可以用於胚胎幹細胞的體內定位。磁力共振波譜可以檢出反映腦組織內生物化學過程的各種代謝產物，包括質子波譜中的N-acetyl aspartate作為神經元標志物，choline作為細胞膜代謝物標志物，myo-inositol作為膠質細胞標志物；磁力共振磷波譜可以提供活體組織生物代謝狀況。除腦病變的診斷外，磁力共振成像和波譜還可以幫助設計治療方案、觀察治療效果及有助於開發新的治療方法。

結論 神經影像技術於觀察腦疾病的形態、新陳代謝、及功能三方面的發展一日千里，此技術可以更有效地診斷及醫治病人。

protons (^{1}H) or ^{31}P, which are normal constituents of endogenous substrates, such as water, lipids, and the main metabolic intermediates. Different pathology and disease processes, such as tumours, oedema, and haemorrhage, are associated with changes in water content and MR relaxation times, and therefore result in different MR contrasts.

In recent years, MR has emerged as the pre-eminent modality which can produce both high-resolution anatomical images and maps that reflect a variety of physiological parameters of the central nervous system at cellular and molecular levels. Besides characterisation of brain disorders, MR can improve the planning and monitoring of therapy and contribute to the development of new therapies. The following is an overview of advanced functional and molecular MR techniques that are currently useful clinically, or have potential clinical uses in the near future.

Dynamic contrast-enhanced magnetic resonance imaging

There are two approaches to the measurement of blood perfusion in the brain with MRI. The first technique is called arterial spin-labelling. This technique makes use of spatially selective inversion or saturation of arterial spins (protons in arterial blood flow) before they enter the region of interest and exchange with tissue water.[1] Arterial spin-labelling is completely non-invasive; however, it is currently hampered by low signal-to-noise ratios in most clinical MR systems. It is expected that with higher field MR systems, the signal-to-noise ratios will improve and clinical application will increase.

The second technique, which is more commonly used, involves the detection of a reduction in signal resulting from the T2* effects of gadolinium-based contrast agent (such as Gd-DTPA) during the passage of a gadolinium bolus through the intracranial vasculature. The magnitude of the decrease in observed signal per voxel is proportional to the concentration of the contrast agent. Dynamic scanning is generally carried out by using T2*-weighted echo-planar imaging at a temporal resolution of 2 seconds or less. From tracer kinetic theory and the tissue response curve deconvolved with the arterial input function, it is possible to calculate: cerebral blood volume (CBV), mean transit time, and cerebral blood flow (CBF).[2,3] Though absolute quantification of these parameters is complicated, even without knowledge of the arterial input function, various semiquantitative parameters pertaining to brain haemodynamics—including maps of relative CBV, relative CBF, mean transit time, and time to peak—can be constructed from the dynamic MRI data. Spatial assessment of multiple haemodynamic parameters can identify brain regions in which the microcirculation is compromised (Fig 1).[4]

Magnetic resonance imaging measurements of CBV are closely associated with tumour grade.[5,6] Many malignant tumours show neovasculature and are more likely to have higher blood flow and blood volume than low-grade tumours. Many malignant gliomas are heterogeneous, and so proper grading of the tumour requires biopsy of the most malignant parts. The increase in local angiogenic activity can be identified by increases in CBV imaged with dynamic MRI, and CBV maps are increasingly used to guide stereotactic biopsies.[7]

Intravenously delivered gadolinium contrast agents go through capillary endothelial membranes and enter the extravascular space. The speed with which this leakage occurs is governed by the surface area of leaky endothelium within the voxel, the permeability of the endothelium, and the concentration gradient of the contrast agent across the vessel wall. Quantification of this leakage can

be performed by dynamic contrast-enhanced T1-weighted imaging techniques and various analyses, which range from simple measures of the rate of enhancement and maximum enhancement, to complex algorithms that apply pharmacokinetic models to the imaging data with the intention of measuring the transfer constant (k^{trans}) of contrast agent between the blood stream and the extracellular space.[8,9] In tissues where blood flow is adequate to deliver contrast agent to the tissues, k^{trans} represents the product of the endothelial permeability and endothelial surface area. Quantification of contrast agent leakage can provide powerful indications about the state of neovascular angiogenesis in tumours and inflammatory tissues. It has even been reported that measurements of K^{trans} can independently predict prognosis in patients with glioblastoma.[10,11] This also has relevance in cancer, where inhibition of angiogenesis presents new therapeutic opportunities by targeting newly formed vessels or inhibition of angiogenic process itself.[12]

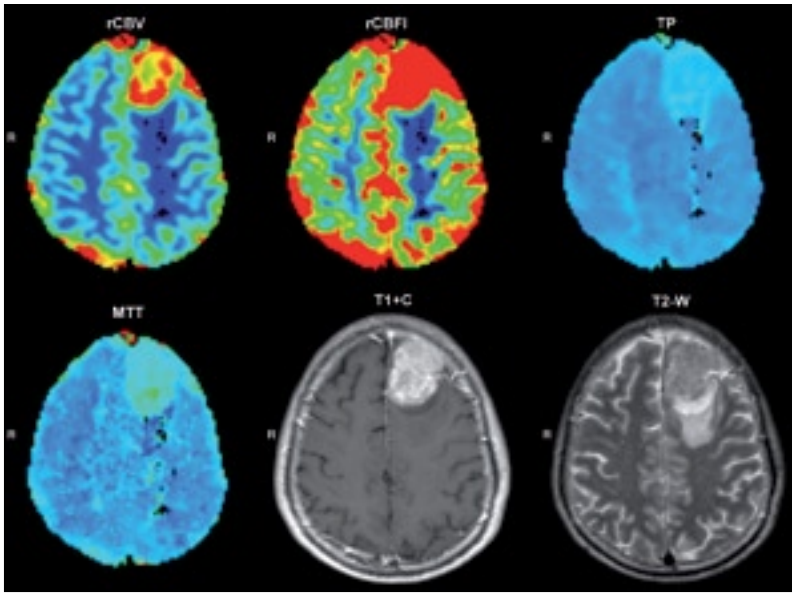

FIG 1. Magnetic resonance perfusion maps in a single section from a patient with a brain tumour in the left frontal lobe
rCBV denotes regional cerebral blood volume; rCBFI regional cerebral blood flow index; TP time to peak; MTT mean transit time. Conventional T1-weighted post-contrast (T1+C) and T2-weighted (T2-W) images acquired at the same plane show that the enhancing portion of the tumour closely matches the region with increased cerebral blood

Blood oxygenation level–dependent magnetic resonance imaging

Blood oxygenation level–dependent (BOLD) MRI is based upon the magnetic property of blood, which is dependent upon the oxygenation state of haemoglobin.[13-15] Deoxygenated haemoglobin is paramagnetic, whereas oxyhaemoglobin is diamagnetic. Deoxygenation results in increased local magnetic susceptibility differences between intravascular and extravascular compartments. Because haemodynamic changes can be monitored directly by MRI, the BOLD effect offers a non-invasive readout of regional brain activity. During neuronal activation in the brain, the local rise in cerebral metabolic rate results in an elevation of both oxygen demand and local CBF. However, the increase in oxygen supply exceeds the increase in oxygen consumption in the activated neuronal network. The consequent increase in local blood oxygenation leads to an increase of BOLD MR signal.

The BOLD MR imaging is a valuable means of studying task-related brain activation in patients with neurological or neuropsychiatric illness. Investigators have used BOLD MR to identify abnormally functioning brain activity during task performance in a variety of patient populations, including those with neurodegenerative, demyelinating, cerebrovascular, and other neurological disorders. It also has an important role in neuro-oncology for the identification of brain areas such as motor and language cortices, that need to be spared during surgical and other tissue-destroying interventions (Fig 2).

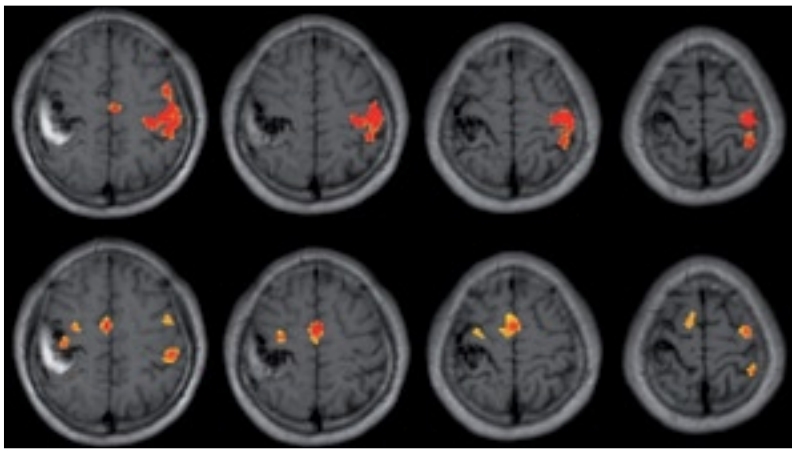

FIG 2. Functional magnetic resonance imaging (MRI) maps obtained from a patient having a pre-surgical motor-cortex assessment
The top row shows the activated areas around the motor cortex when the patient performed a right-hand sponge squeezing task. The bottom row shows a different pattern of activation when the patient performed the same task using his left hand. Tumour invasion in the right motor cortex and displaced activated areas can be clearly identified from the images

As BOLD MRI is sensitive to changes in the regional tissue oxygenation status, it can be used to monitor acute deoxygenation after induction of ischaemia as well as reoxygenation after reperfusion. The BOLD MRI may provide tools to differentiate between irreversibly damaged brain areas and tissue in jeopardy. The BOLD MRI studies of stroke patients have shown that the laterality of primary sensorimotor cortex activation may shift after an infarct from typical contralateral organisation toward the side ipsilateral to movement, in a process known as plasticity.

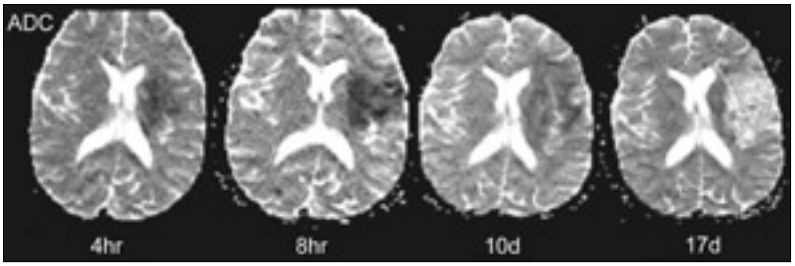

FIG 3. Time course of an ischaemic infarction shown on apparent diffusion coefficient (ADC) images

Serial images demonstrate the evolution of a left middle cerebral artery infarction. At 4 hours, the lesion is hypointense on the ADC image. At 8 hours, the lesion has increased in size and the region initially visualised has become more hypointense on ADC image. At 10 days, the ADC of most of the infarct has pseudonormalised and the lesion is close to isointense to normal brain tissue. At 17 days, the ADC is predominantly elevated and appears hyperintense on the ADC image. The left caudate head (with low ADC) has an acute infarct (reproduced with permission from Schaefer[25])

The BOLD MRI can also be used in the study of progressive neurological diseases at the point of subtle neuronal dysfunction, prior to overt anatomic pathology. Given the growing body of evidence that alterations in synaptic function are present very early in the pathophysiological process of Alzheimer's disease and related disorders, it is possible that BOLD MRI may be useful in detecting alterations in brain function, long before the development of clinical symptoms and significant neuropathology. In clinical populations, it has also been applied to investigate cocaine dependence, depression, schizophrenia, and Parkinson's disease. The BOLD MRI has also been shown to reveal regional brain activation responses associated with individual differences in behavioural response to pharmacological agents.

Diffusion-weighted magnetic resonance imaging

Diffusion-weighted (DW) MRI allows the measurement of random Brownian movement (self-diffusion) of MR-detectable molecules such as the microscopical motion of tissue water.[16] Diffusion-weighted MRI measures all incoherent motions inside a voxel, and motion in tissue is influenced by various factors such as: local barriers (eg cell membranes), transport processes, and adsorption to macromolecules. Therefore in-vivo DW MRI does not actually measure the intrinsic self-diffusion of water molecules. In the clinical practice, apparent diffusion rather than actual water diffusion is measured. This is quantitatively expressed by the so-called apparent diffusion coefficient (ADC). Most clinical DW MR examinations generate both DW MRIs and ADC maps. Diffusion restriction (reduction) areas appear bright on DW MRIs and dark on ADC map. Diffusion-weighted MRI has been proven to be sensitive to cellular changes and tissue abnormalities at an even earlier stage.

Reduction of ADC in ischaemia is due to a shift of extracellular water into intracellular compartments as a result of disrupted ion homeostasis.[17] In the extracellular space, water diffuses relatively freely; in intracellular compartments, there is a high density of diffusional barriers and restrictions due to the presence of cellular membranes. Animal models demonstrate a reduction in Na+/K+ ATPase activity and cytotoxic oedema due to acute hyponatremic encephalopathy also results in restricted diffusion.[18]

Diffusion-weighted MRI is very sensitive and specific in detecting hyperacute and acute infarctions. In adult humans, restricted diffusion has been observed as early as 30 minutes after an acute neurological deficit. In the time course, the ADC of affected brain tissue continues to decrease, reaching its nadir 8 to 32 hours post-infarction, and remains significantly reduced for 3 to 5 days. It is believed that a reduction of the ADC by more than 20% leads to irreversible tissue damage.[19] With the development of vasogenic oedema and cell membrane disruption leading to an increase in extracellular water, the ADC begins to rise. The ADC pseudonormalises at 1 to 4 weeks. With continued increase in extracellular water, tissue cavitation and gliosis, the ADC then remains elevated indefinitely (Fig 3). Together with perfusion imaging, DW MRI is useful in predicting final infarct size and patient outcome. Following arterial occlusion, brain regions with both decreased diffusion and decreased perfusion are thought to represent non-viable tissue (the infarction core). The peripheral region, characterised by normal diffusion and decreased perfusion, represents what amounts to an 'ischaemic penumbra' or area at risk for infarction.[20,21] It has been reported that baseline perfusion MRI/DW MRI mismatch can identify subgroups that are likely to benefit from thrombolysis treatment and can potentially also identify subgroups that are unlikely to benefit.[22] In the meantime, a recent systematic review suggested that current data available on perfusion MRI/DW MRI mismatch are too limited to guide thrombolysis in routine practice, and that better definitions of mismatch and more data are needed to determine its role.[23]

Diffusion-weighted MRI also allows the differentiation of chronic lesions from acute lesions, which is difficult with conventional techniques.[24] Diffusion-weighted MRI may also parallel the severity of clinical neurologic deficits. There is a significant correlation between the acute ADC ratio (ADC of lesion/ADC of normal contralateral brain) and chronic neurologic assessment scales.[25]

Most brain tumours such as gliomas demonstrate an elevated ADC in comparison to normal brain tissue. Cystic, necrotic, and oedematous tissue in and near brain tumours can be identified as areas with high ADC values. Tumours with dense cell packing such as lymphomas and medulloblastomas

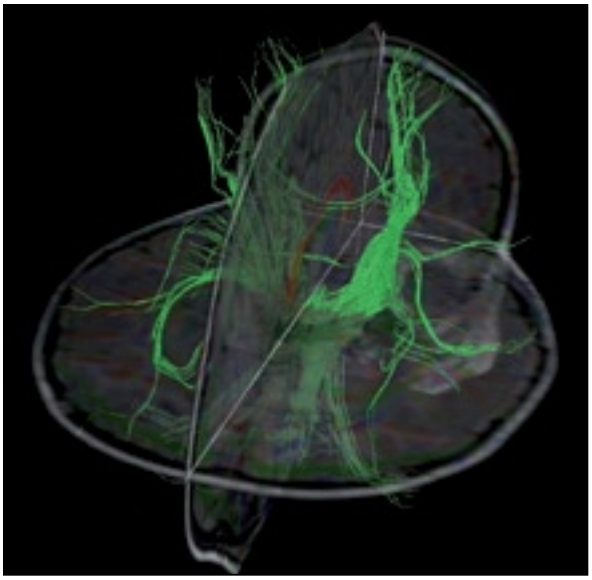

FIG 4. A magnetic resonance (MR) tractography image from a healthy subject using a 3.0 Tesla scanner
Diffusion tensor MR images were acquired using a 32-diffusion gradient scheme with a total scanning time of about 7 minutes

may demonstrate a restricted ADC. Diffusion-weighted MRI may allow the differentiation of brain abscess from necrotic or cystic brain tumour. Abscess cavities and empyemas have restricted diffusion, probably due to the high cellularity and viscosity of pus. Diffusion-weighted MRI signal intensities in abscess cavities are markedly higher and ADC ratios (comparisons with normal brain tissue) are lower than those of necrotic tumours.[25,26]

More recently, DW MRI has been used to monitor response to therapy. The ADC of gliomas increases significantly after treatment due to destruction of tumour cells, widening of the extracellular space, and a consequent increase in extracellular and therefore relatively mobile water.[27] The magnitude of change in the ADC within brain tumours after a course of radiotherapy predicts their clinical progression.[27-29]

With cross-sectional studies, it is reported that DW MRI–derived parameters in multiple sclerosis show significant correlations with clinical findings, suggesting that they might serve as additional measures of outcome when monitoring evolution of the disease in patients.[30-32]

Diffusion tensor magnetic resonance imaging

Because of the organised structure of tissues, there is variation in water diffusion in different directions, such diffusion is termed anisotropic. Anisotropy in tissue structure leads to anisotropy in water diffusion that can be measured by the MRI technique termed diffusion tensor (DT) imaging. The water molecules in axonal tracts are more likely to diffuse along the tract than in directions perpendicular to it. Thus, MRI can be used to evaluate the integrity of axonal fibres in vivo in normal and in diseased brain tissues.[32-34] Excellent agreement has been noted between fibre maps using DT MRI and known axonal projections (Fig 4).[33,34] Many developmental, ageing, and pathological processes of the brain influence the microstructural composition and architecture of affected tissues. The diffusion of water within tissues is altered by changes in the tissue microstructure and organisation; consequently, DT MRI is a potentially powerful probe for characterising the effects of disease and ageing on brain microstructure.

It has been demonstrated that parallel organisation of white matter fibre bundles is the basis for diffusion anisotropy, whereas myelin appears to modulate the amount of anisotropy.[35] Nearly all studies of myelination with normal brain development and demyelination with disease-related processes have found less diffusion anisotropy whenever axons are less myelinated.[36] In multiple sclerosis, Pagani et al[37] used tractography on healthy volunteers to create a probability map for the pyramidal tract, which was then applied to patients to calculate DT MRI–derived metrics inside their pyramidal tracts. They found that lesion volume and mean diffusivity of the pyramidal tract correlated well with clinical symptoms related to motor function, whereas these metrics were unchanged in patients without motor function symptoms.

Another common application of DT MRI is to characterise white matter in patients with brain tumours. Brain tumour infiltration may cause alterations in white matter fibre orientation.[38] Diffusion tensor MRI can be used for mapping of white matter anatomy prior to surgery. This assists neurosurgeons in localising critical white matter pathways, enabling minimisation of damage. In addition to visualisation of white matter tracts, DT MRI has been used to study the effects of surgery on white matter pathways. Diffusion tensor MRI also offers promise as a means of following the response to stem cell therapies in the central nervous system.[39]

Two recent studies have examined the relationships between DT MRI changes from radiation and cognitive function (as measured by IQ).[40,41] Both reported a correlation between decreased fractional anisotropy and decreased IQ.

Magnetisation transfer magnetic resonance imaging

Magnetisation transfer (MT) effects are caused by chemical exchange or dipole-dipole interactions between protons from water and macromolecules. The very broad MR signal from protons of

macromolecules and immobile water can be suppressed by off-resonance, frequency-selective radiofrequency irradiation. This phenomenon does not affect the narrow MR signal from mobile water molecules. Saturation of the immobile proton pool causes a reduction in signal from the free water pool via chemical exchange and cross-relaxation. Thus the MT effect (measured as MT ratio [MTR]=[S0 – Ss]/S0, where S0 and Ss are the signal intensities before and after saturation, respectively) yields information on: the ratio between free and bound proton pools, the rate of magnetisation exchange, and the magnetic properties of the immobilised proton pool.

Magnetisation transfer MRI has been successfully applied to pathologies that alter the structural integrity of brain tissue.[42] The dynamics of MT changes can correlate with the extent of demyelination and remyelination.[43] Though decrease in MTR is a non-specific sign of myelin loss and axon damage in multiple sclerosis, MTR imaging plays an important role as a surrogate marker of myelin repair, because recovery has been shown to correlate with remyelination.[44,45] Magnetisation transfer imaging may help to predict an individual's clinical course, as well as the effects of treatment, by revealing evidence of myelin repair and neuroprotection. Chen et al[46] reported that the use of voxel-wise longitudinal comparison allows lesion chronology classification into new, stable, and resolved. Agosta et al[47] reported that early MTR abnormalities in normal-appearing brain tissue can predict the clinical evolution of multiple sclerosis. A modest-to-strong correlation was found between baseline MTR and subsequent change in the Expanded Disability Status Scale,[48] such that MT MRI metrics have been shown to correlate with the degree of disability.

In patients with traumatic brain injury, MT contrast was significantly reduced in regions with diffuse axonal injury.[49] In such patients, MT MRI detects the presence of microstructural tissue damage in susceptible regions and relates to axonal damage (such as in the pons and the splenium of the corpus callosum), even when there is no MRI-detectable intracerebral lesion.[50,51]

Evidently MT MRI measures derived from the whole of the brain, as well as those from the temporal and frontal lobes in isolation, correlate strongly with global cognitive deterioration and impairment of functions in both Alzheimer's disease and mild cognitive impairment.[52] Moreover, structural brain changes may even be present before the onset of cognitive deficits.[53]

In cerebral ischaemia, a reduction in MTR may be related to breakdown of macromolecular tissue components and vasogenic oedema-associated increases in free interstitial water.[54] Reduced MTR values have been demonstrated in chronic ischaemic lesions, suggesting a role for MT MRI in estimating the age of cerebral infarcts.[55]

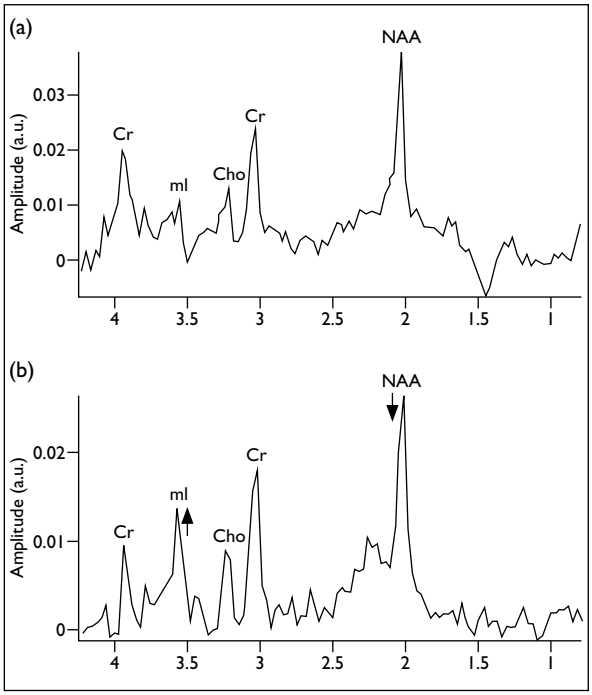

FIG 5. Representative proton spectra acquired at 1.5 T using the point-resolved spectroscopy sequence (PRESS) at a short TE of 30 ms in the occipital lobe region

(a) The spectrum from a subject without cognitive dysfunctions showing metabolites such as N-acetylaspartate (NAA), choline (Cho), creatine (Cr), myo-inositol (ml) within normal ranges. (b) The spectrum from a patient with Alzheimer's disease showing a different pattern of metabolites; the amount of ml is markedly increased and the level of NAA is reduced compared with normal values

Magnetic resonance spectroscopy

In the proton (^{1}H) MRS involving long echo times, commonly identifiable metabolite peaks include those of N-acetylaspartate (NAA), lactate, choline (Cho), and creatine (Cr) [Fig 5]. N-acetylaspartate is contained almost exclusively within neurons and is therefore considered to be an in-vivo marker of neuronal viability. Lactate is the end product of glycolysis, which can accumulate in the brain when tissue becomes ischaemic. Activated inflammatory macrophages can also produce high levels of lactate. The Cho peak arises from Cho-containing compounds, including: Cho, phosphocholine, glycerophosphocholine, and betaine. An elevated Cho peak indicates increased cell membrane turnover, as occurs in neoplastic processes. The Cr peak is constituted by at least two compounds, Cr and phosphocreatine. Many studies use the level of the Cr peak as an internal reference, because it is regarded as relatively constant throughout the brain and does not change in most pathologies.

The MRS peaks can be quantified absolutely or semi-quantitatively. Relative concentrations are usually expressed as metabolite-to-Cr ratios. The calculation of absolute concentrations requires correction for many factors, including the adjustments for T1 and T2 relaxation effects, and referencing the results to a known internal standard (such as the unsuppressed regional brain water signal,[56] or an external standard of known concentration[57,58]).

Proton MR spectroscopy is used to evaluate brain tumours in routine clinical practice. In most brain tumours, neuronal elements and hence NAA concentrations are low and thus the Cho-to-NAA ratio is high.[59] Malignant gliomas show metabolic changes on proton MRS that differentiate them from low-grade gliomas and other brain lesions.[60] High lipid and Cho peaks are associated with histological indicators of malignancy (cellular anaplastic features and nuclear density).[61] A high lactate concentration seen with MRS may be associated with non-oxidative glycolysis in gliomas.[62] The ability of proton MR spectroscopy to distinguish tumours from radiation necrosis, benign lesions, or oedema is extremely important in clinical practice. Proton MRS has also been used successfully to monitor the effects of therapy for brain tumours.[63-65] Therapeutic intervention, particularly radiation therapy, can induce delayed necrosis in brain tumours. Necrosis might be associated with a mass effect together with contrast enhancement and has a similar appearance to recurrent malignant tumours visualised by standard structural imaging. The MRS is capable of distinguishing residual or recurrent tumours from pure radiation necrosis.[66]

Analysis of metabolic profiles using proton MRS has been proposed as a sensitive methodology to detect neurodegenerative processes. In the case of Alzheimer's disease, Miller et al[67] reported an analysis based on signals of myo-inositol and NAA. Magnetic resonance spectra of patients suffering from mild cognitive impairment contained a myo-inositol signal of increased intensity as the only alteration to the spectrum as compared to an age-matched control. In patients with confirmed Alzheimer's disease, the signal of myo-inositol remained elevated while the NAA peak was significantly decreased. Their report has been followed by a host of others showing reproducible patterns of decreased NAA and increased myo-inositol in the occipital, temporal, parietal, and frontal regions of patients with Alzheimer's disease, even in the early stages.[68] These spectral alterations can be used to differentiate patients with suspected Alzheimer's disease from normal elderly, as well as patients with other kinds of dementias.[69]

In epilepsy patients, it has been shown that there is a reduction of the NAA signal, with an increase in the Cr signal as well as an increase in the Cho signal in the temporal lobes ipsilateral to the seizure focus.[70] Proton MRS provides useful information in the preoperative investigation of patients with temporal lobe epilepsy. It contributes to lateralisation and detection of bilateral abnormalities (noted in more than 40% of cases). Correlation between proton MRS alterations and the severity of the epilepsy has also been noted. In patients who show no obvious changes on MRI (approximately 30% with temporal lobe epilepsy), MRS can identify the affected hemisphere in the majority (based on reductions in NAA and elevations in Cho). Proton MRS can also be used to predict surgical outcomes, because patients with an ipsilateral abnormality have a much better chance of a seizure-free outcome than those with bilateral abnormalities.[71,72]

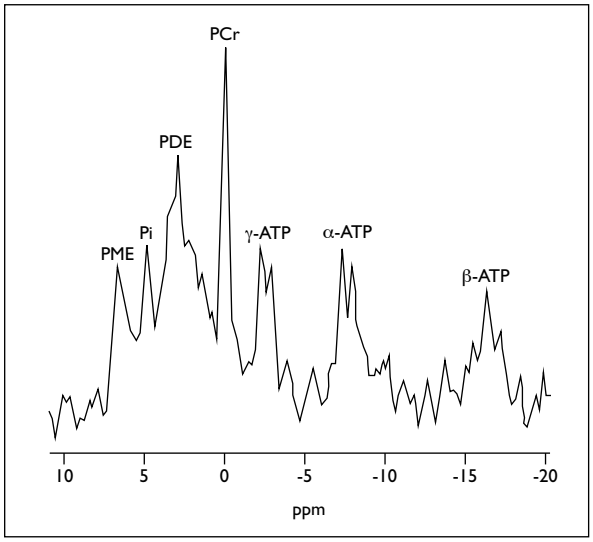

FIG 6. Typical ^{31}P spectrum from the temporo-occipital cortex in a normal volunteer (voxel size 3×3×3 cm^3) at 1.5 T using a transmit-receive head coil

Peaks correspond to metabolites; phosphomonoesters (PME); phosphodiesters (PDE); phosphocreatine (PCr); inorganic phosphate (Pi); and the α, β, and γ groups of adenosine trinucleotide phosphate (ATP)

Proton MR spectroscopy has also been applied to other brain diseases, such as demyelination conditions. In both cross-sectional and longitudinal studies of multiple sclerosis, a decrease in NAA:Cr ratio has a very strong correlation with disability.[73]

Phosphorous (^{31}P) MRS has also been used to study high-energy phosphate metabolites. The major peaks evident on the ^{31}P MRS include α, β, and γ nucleotide triphosphates which reflect adenosine trinucleotide phosphate levels, phosphocreatine (an indicator of oxidative metabolism), phosphodiesters and phosphomonoesters (related to cell membranes), and inorganic phosphate (Fig 6). From the phosphorus spectroscopy, intracellular pH can also be derived, providing information for the management of severe metabolic disturbances.

Cellular magnetic resonance imaging

Cellular MR imaging in the brain can be carried out with cells labelled with an MR contrast agent. This can be performed ex-vivo by labelling of cells with superparamagnetic iron oxide (SPIO) or ultra-small SPIO (USPIO) contrast agents and then implanting them into the brain, or after intravenous injection of USPIO agents.[74-76] Following intravenous injection, SPIO/USPIO is recognised by macrophages as antigens and will be incorporated into the lysosomes via endocytosis. Macrophages labelled with SPIO/USPIO cause significant changes of local parenchymal T2/T2* relaxation rates. The uptake of SPIO and USPIO nanoparticles by phagocytic monocytes and macrophages provides a valuable in-vivo tool by which MRI can be used to monitor involvement of macrophages in inflammatory processes, such as multiple sclerosis, traumatic nerve injury, stroke, and brain tumours.

Saleh et al[77] performed an MRI study with USPIO in 10 ischaemic stroke patients; USPIO was administered intravenously; MRI scans performed 24 h and 48 h later revealed signal alterations in all 10 patients. For multiple sclerosis, Dousset et al[78] used USPIO to demonstrate visualisation of macrophage activity in patients with relapsing–remitting multiple sclerosis. It is known that activation of microglia and infiltration of immune cells across the blood brain barrier are triggers for the development of inflammatory plaques in multiple sclerosis. Imaging might therefore characterise a distinct cellular and inflammatory event in the pathogenesis of multiple sclerosis lesions. Neuwelt et al[79] conducted clinical studies with MRI monitoring of macrophages in brain tumours. They showed that most patients given USPIO had MRI-signal alterations, which reflect the presence of iron oxide particles in the tumour.[79,80] It was hypothesised that viable cells (but not for necrotic tissue) at the tumour margin are able to engulf such particles. The macrophage MRI detection with USPIO of tumour morphology might therefore facilitate the surgical resection or biopsy of brain tumours.

Recently the therapeutic use of stem and progenitor cells as a substitute for malfunctioning endogenous cell populations has received considerable attention in brain disorders, such as stroke, trauma, demyelinating diseases, and tumours. The development of stem cell–based therapies requires a quantitative and qualitative assessment of their distribution to target organs and their engraftment. To be visualised, these progenitor cells must be labelled with an intracellular tracer that can be detected by MR imaging. Due to its high MR relaxivity and low toxicity, SPIO/USPIO has been considered to be such an agent of choice.[71,72] It is now possible to incorporate sufficient amounts of SPIO/USPIO into stem cells, enabling their detection by MRI in vivo.[81-83]

Acknowledgement

The authors thank David KW Yeung at the Prince of Wales Hospital, Hong Kong, for providing some of the MRI figures used in this paper.

References

1. Detre JA, Leigh JS, Williams DS, Koretsky AP. Perfusion imaging. Magn Reson Med 1992;23:37-45.
2. Meier P, Zierler KL. On the theory of the indicator-dilution method for measurement of blood flow and volume. J Appl Physiol 1954;6:731-44.
3. Rosen BR, Belliveau JW, Vevea JM, Brady TJ. Perfusion imaging with NMR contrast agents. Magn Reson Med 1990;14:249-65.
4. Roberts TP, Vexler Z, Derugin N, Moseley ME, Kucharczyk J. High-speed MR imaging of ischemic brain injury following stenosis of the middle cerebral artery. J Cereb Blood Flow Metab 1993;13:940-6.
5. Law M, Oh S, Babb JS, et al. Low-grade gliomas: dynamic susceptibility-weighted contrast-enhanced perfusion MR imaging—prediction of patient clinical response. Radiology 2006;238:658-67.
6. Maia AC Jr, Malheiros SM, da Rocha AJ, et al. MR cerebral blood volume maps correlated with vascular endothelial growth factor expression and tumor grade in nonenhancing gliomas. AJNR Am J Neuroradiol 2005;26:777-83.
7. Aronen HJ, Pardo FS, Kennedy DN, et al. High microvascular blood volume is associated with high glucose uptake and tumor angiogenesis in human gliomas. Clin Cancer Res 2000;6:2189-200.
8. Tofts PS. Modeling tracer kinetics in dynamic Gd-DTPA MR imaging. J Magn Reson Imaging 1997;7:91-101.
9. Jackson A. Analysis of dynamic contrast enhanced MRI. Br J Radiol 2004;77(Spec No 2):154S-166S.
10. Mills SJ, Patankar TA, Haroon HA, Balériaux D, Swindell R, Jackson A. Do cerebral blood volume and contrast transfer coefficient predict prognosis in human glioma? AJNR Am J Neuroradiol 2006;27:853-8.
11. Patankar TF, Haroon HA, Mills SJ, et al. Is volume transfer coefficient (K(trans)) related to histologic grade in human gliomas? AJNR Am J Neuroradiol 2005;26:2455-65.
12. Leach MO, Brindle KM, Evelhoch JL, et al. Assessment of antiangiogenic and antivascular therapeutics using MRI: recommendations for appropriate methodology for clinical trials. Br J Radiol 2003;76(Spec No 1):87S-91S.
13. Ogawa S, Tank DW, Menon R, et al. Intrinsic signal changes accompanying sensory stimulation: functional brain mapping with magnetic resonance imaging. Proc Natl Acad Sci USA 1992;89:5951-5.
14. Ogawa S, Lee TM, Nayak AS, Glynn P. Oxygenation-sensitive

contrast in magnetic resonance image of rodent brain at high magnetic fields. Magn Reson Med 1990;14:68-78.
15. Mandeville JB, Rosen BR. Functional MRI. In: Toga AW, Mazziotta JC, editors. Brain mapping: the methods. 2nd ed. London: Academic Press; 2002: 315-49.
16. Le Bihan D, Breton E, Lallemand D, Aubin ML, Vignaud J, Laval-Jeantet M. Separation of diffusion and perfusion in intravoxel incoherent motion MR imaging. Radiology 1988;168:497-505.
17. Moseley ME, Cohen Y, Mintorovitch J, et al. Early detection of regional cerebral ischemia in cats: comparison of diffusion- and T2-weighted MRI and spectroscopy. Magn Reson Med 1990;14:330-46.
18. Verheul HB, Balázs R, Berkelbach van der Sprenkel JW, Tulleken CA, Nicolay K, van Lookeren Campagne M. Temporal evolution of NMDA-induced excitoxicity in the neonatal rat brain measured with 1H nuclear magnetic resonance imaging. Brain Res 1993;618:203-12.
19. Hoehn-Berlage M, Eis M, Back T, Kohno K, Yamshita K. Changes of relaxation times (T1, T2) and apparent diffusion coefficient after permanent middle cerebral artery occlusion in the rat: temporal evolution, regional extent, and comparison with histology. Magn Reson Med 1995;34:824-34.
20. Neumann-Haefelin T, Wittsack HJ, Wenserski F, et al. Diffusion- and perfusion-weighted MRI. The DWI/PWI mismatch region in acute stroke. Stroke 1999;30:1591-7.
21. Hossmann KA, Hoehn-Berlage M. Diffusion and perfusion MR imaging of cerebral ischemia. Cerebrovasc Brain Metab Rev 1995;7:187-217.
22. Albers GW, Thijs VN, Wechsler L, et al. Magnetic resonance imaging profiles predict clinical response to early reperfusion: the diffusion and perfusion imaging evaluation for understanding stroke evolution (DEFUSE) study. Ann Neurol 2006;60:508-17.
23. Kane I, Sandercock P, Wardlaw J. Magnetic resonance perfusion diffusion mismatch and thrombolysis in acute ischaemic stroke: a systematic review of the evidence to date. J Neurol Neurosurg Psychiatry 2007;78:485-91.
24. Singer MB, Chong J, Lu D, Schonewille WJ, Tuhrim S, Atlas SW. Diffusion-weighted MRI in acute subcortical infarction. Stroke 1998;29:133-6.
25. Schaefer PW. Applications of DWI in clinical neurology. J Neurol Sci 2001;186(Suppl 1):25S-35S.
26. Kim YJ, Chang KH, Song IC, et al. Brain abscess and necrotic or cystic brain tumor: discrimination with signal intensity on diffusion-weighted MR imaging. AJR Am J Roentgenol 1998;171:1487-90.
27. Hamstra DA, Chenevert TL, Moffat BA, et al. Evaluation of the functional diffusion map as an early biomarker of time-to-progression and overall survival in high-grade glioma. Proc Natl Acad Sci USA 2005;102:16759-64.
28. Moffat BA, Chenevert TL, Lawrence TS, et al. Functional diffusion map: a noninvasive MRI biomarker for early stratification of clinical brain tumor response. Proc Natl Acad Sci USA 2005;102:5524-9.
29. Heide AC, Richards TL, Alvord EC Jr, Peterson J, Rose LM. Diffusion imaging of experimental allergic encephalomyelitis. Magn Reson Med 1993;29:478-84.
30. Benedict RH, Bruce J, Dwyer MG, et al. Diffusion-weighted imaging predicts cognitive impairment in multiple sclerosis. Mult Scler 2007;13:722-30.
31. Cercignani M, Inglese M, Pagani E, Comi G, Filippi M. Mean diffusivity and fractional anisotropy histograms of patients with multiple sclerosis. AJNR Am J Neuroradiol 2001;22:952-8.
32. Mori S, Itoh R, Zhang J, et al. Diffusion tensor imaging of the developing mouse brain. Magn Reson Med 2001;46:18-23.
33. Basser PJ, Pajevic S, Pierpaoli C, Duda J, Aldroubi A. In vivo fiber tractography using DT-MRI data. Magn Reson Med 2000;44:625-32.
34. Kindlmann G, Weinstein D, Hart D. Strategies for direct volume rendering of diffusion tensor fields. IEEE Trans Vis Comput Graph 2000;6:124-38.
35. Song SK, Sun SW, Ramsbottom MJ, Chang C, Russell J, Cross AH. Dysmyelination revealed through MRI as increased radial (but unchanged axial) diffusion of water. Neuroimage 2002;17:1429-36.
36. Rovaris M, Gass A, Bammer R, et al. Diffusion MRI in multiple sclerosis. Neurology 2005;65:1526-32.
37. Pagani E, Filippi M, Rocca MA, Horsfield MA. A method for obtaining tract-specific diffusion tensor MRI measurements in the presence of disease: application to patients with clinically isolated syndromes suggestive of multiple sclerosis. Neuroimage 2005;26:258-65.
38. Field AS, Alexander AL. Diffusion tensor imaging in cerebral tumor diagnosis and therapy. Top Magn Reson Imaging 2004;15:315-24.
39. Jiang Q, Zhang ZG, Ding GL, et al. MRI detects white matter reorganization after neural progenitor cell treatment of stroke. Neuroimage 2006;32:1080-9.
40. Mabbott DJ, Noseworthy MD, Bouffet E, Rockel C, Laughlin S. Diffusion tensor imaging of white matter after cranial radiation in children for medulloblastoma: correlation with IQ. Neuro Oncol 2006;8:244-52.
41. Khong PL, Leung LH, Fung AS, et al. White matter anisotropy in post-treatment childhood cancer survivors: preliminary evidence of association with neurocognitive function. J Clin Oncol 2006;24:884-90.
42. Filippi M, Rocca MA. Magnetization transfer magnetic resonance imaging of the brain, spinal cord, and optic nerve. Neurotherapeutics 2007;4:401-13.
43. Rademacher J, Engelbrecht V, Bürgel U, Freund H, Zilles K. Measuring in vivo myelination of human white matter fiber tracts with magnetization transfer MR. Neuroimage 1999;9:393-406.
44. Deloire-Grassin MS, Brochet B, Quesson B, et al. In vivo evaluation of remyelination in rat brain by magnetization transfer imaging. J Neurol Sci 2000;178:10-6.
45. Zivadinov R. Can imaging techniques measure neuroprotection and remyelination in multiple sclerosis? Neurology 2007;68(22 Suppl 3):72S-82S.
46. Chen JT, Collins DL, Freedman MS, et al. Local magnetization transfer ratio signal inhomogeneity is related to subsequent change in MTR in lesions and normal-appearing white-matter of multiple sclerosis patients. Neuroimage 2005;25:1272-8.
47. Agosta F, Rovaris M, Pagani E, Sormani MP, Comi G, Filippi M. Magnetization transfer MRI metrics predict the accumulation of disability 8 years later in patients with multiple sclerosis. Brain 2006;129:2620-7.
48. Rovaris M, Agosta F, Sormani MP, et al. Conventional and magnetization transfer MRI predictors of clinical multiple sclerosis evolution: a medium-term follow-up study. Brain 2003;126:2323-32.

49. Smith DH, Meaney DF, Lenkinski RE, et al. New magnetic resonance imaging techniques for the evaluation of traumatic brain injury. J Neurotrauma 1995;12:573-7.
50. Bagley LJ, McGowan JC, Grossman RI, et al. Magnetization transfer imaging of traumatic brain injury. J Magn Reson Imaging 2000;11:1-8.
51. McGowan JC, Yang JH, Plotkin RC, et al. Magnetization transfer imaging in the detection of injury associated with mild head trauma. AJNR Am J Neuroradiol 2000;21:875-80.
52. van der Flier WM, van den Heuvel DM, Weverling-Rijnsburger AW, et al. Magnetization transfer imaging in normal aging, mild cognitive impairment, and Alzheimer's disease. Ann Neurol 2002;52:62-7.
53. van Es AC, van der Flier WM, Admiraal-Behloul F, et al. Magnetization transfer imaging of gray and white matter in mild cognitive impairment and Alzheimer's disease. Neurobiol Aging 2006;27:1757-62.
54. Ordidge RJ, Helpern JA, Knight RA, Qing ZX, Welch KM. Investigation of cerebral ischemia using magnetization transfer contrast (MTC) MR imaging. Magn Reson Imaging 1991;9:895-902.
55. Hanyu H, Imon Y, Sakurai H, et al. Diffusion-weighted magnetic resonance and magnetization transfer imaging in the assessment of ischemic human stroke. Intern Med 1998;37:360-5.
56. Christiansen P, Henriksen O, Stubgaard M, Gideon P, Larsson HB. In vivo quantification of brain metabolites by 1H-MRS using water as an internal standard. Magn Reson Imaging 1993;11:107-18.
57. Michaelis T, Merboldt KD, Bruhn H, Hänicke W, Frahm J. Absolute concentrations of metabolites in the adult human brain in vivo: quantification of localized proton MR spectra. Radiology 1993;187:219-27.
58. Jansen JF, Backes WH, Nicolay K, Kooi ME. 1H MR spectroscopy of the brain: absolute quantification of metabolites. Radiology 2006;240:318-32.
59. Hollingworth W, Medina LS, Lenkinski RE, et al. A systematic literature review of magnetic resonance spectroscopy for the characterization of brain tumors. AJNR Am J Neuroradiol 2006;27:1404-11.
60. Law M, Yang S, Wang H, et al. Glioma grading: sensitivity, specificity, and predictive values of perfusion MR imaging and proton MR spectroscopic imaging compared with conventional MR imaging. AJNR Am J Neuroradiol 2003;24:1989-98.
61. Möller-Hartmann W, Herminghaus S, Krings T, et al. Clinical application of proton magnetic resonance spectroscopy in the diagnosis of intracranial mass lesions. Neuroradiology 2002;44:371-81.
62. Herholz K, Heindel W, Luyten PR, et al. In vivo imaging of glucose consumption and lactate concentration in human gliomas. Ann Neurol 1992;31:319-27.
63. Murphy PS, Viviers L, Abson C, et al. Monitoring temozolomide treatment of low-grade glioma with proton magnetic resonance spectroscopy. Br J Cancer 2004;90:781-6.
64. Hall WA, Truwit CL. 1.5 T: spectroscopy-supported brain biopsy. Neurosurg Clin N Am 2005;16:165-72.
65. Rock JP, Scarpace L, Hearshen D, et al. Associations among magnetic resonance spectroscopy, apparent diffusion coefficients, and image-guided histopathology with special attention to radiation necrosis. Neurosurgery 2004;54:1111-9.
66. Graves EE, Pirzkall A, Nelson SJ, Larson D, Verhey L. Registration of magnetic resonance spectroscopic imaging to computed tomography for radiotherapy treatment planning. Med Phys 2001;28:2489-96.
67. Miller BL, Moats RA, Shonk T, Ernst T, Wolley S, Ross BD. Alzheimer disease: depiction of increased cerebral myo-inositol with proton MR spectroscopy. Radiology 1993;187:433-7.
68. Rosena Y, Lenkinski RE. Recent advances in magnetic resonance neurospectroscopy. Neurotherapeutics 2007;4:330-45.
69. Kantarci K, Petersen RC, Boeve BF, et al. 1H MR spectroscopy in common dementias. Neurology 2004;63:1393-8.
70. Connelly A, Jackson GD, Duncan JS, King MD, Gadian DG. Magnetic resonance spectroscopy in temporal lobe epilepsy. Neurology 1994;44:1411-7.
71. Willmann O, Wennberg R, May T, Woermann FG, Pohlmann-Eden B. The role of 1H magnetic resonance spectroscopy in pre-operative evaluation for epilepsy surgery. A meta-analysis. Epilepsy Res 2006;71:149-58.
72. Hammen T, Kerling F, Schwarz M, et al. Identifying the affected hemisphere by (1)H-MR spectroscopy in patients with temporal lobe epilepsy and no pathological findings in high resolution MRI. Eur J Neurol 2006;13:482-90.
73. Narayana PA. Magnetic resonance spectroscopy in the monitoring of multiple sclerosis. J Neuroimaging 2005;15(4 Suppl):46S-57S.
74. Petry KG, Boiziau C, Dousset V, Brochet B. Magnetic resonance imaging of human brain macrophage infiltration. Neurotherapeutics 2007;4:434-42.
75. Wang YX, Hussain SM, Krestin GP. Superparamagnetic iron oxide contrast agents: physiochemical characteristics and applications in MR imaging. Eur Radol 2001;11:2319-31.
76. Corot C, Robert P, Idée JM, Port M. Recent advances in iron oxide nanocrystal technology for medical imaging. Adv Drug Deliv Rev 2006;58:1471-504.
77. Saleh A, Schroeter M, Jonkmanns C, Hartung HP, Mödder U, Jander S. In vivo MRI of brain inflammation in human ischaemic stroke. Brain 2004;127:1670-7.
78. Dousset V, Brochet B, Deloire MS, et al. MR imaging of relapsing multiple sclerosis patients using ultra-small-particle iron oxide and compared with gadolinium. AJNR Am J Neuroradiol 2006;27:1000-5.
79. Neuwelt EA, Várallyay P, Bagó AG, Muldoon LL, Nesbit G, Nixon R. Imaging of iron oxide nanoparticles by MR and light microscopy in patients with malignant brain tumours. Neuropathol Appl Neurobiol 2004;30:456-71.
80. Varallyay P, Nesbit G, Muldoon LL, et al. Comparison of two superparamagnetic viral-sized iron oxide particles ferumoxides and ferumoxtran-10 with a gadolinium chelate in imaging intracranial tumors. AJNR Am J Neuroradiol 2002;23:510-9.
81. Bulte JW, Kraitchman DL. Iron oxide MR contrast agents for molecular and cellular imaging. NMR Biomed 2004;17:484-99.
82. Bulte JW, Duncan ID, Frank JA. In vivo magnetic resonance tracking of magnetically labeled cells after transplantation. J Cereb Blood Flow Metab 2002;22:899-907.
83. Zhu J, Zhou L, XingWu F. Tracking neural stem cells in patients with brain trauma. N Engl J Med 2006;355:2376-8.